A Dynamical State Space Representation and Performance Analysis of a Feedback-Controlled Rotary Left Ventricular Assist Device

Marwan A. Simaan, *Fellow, IEEE*, Antonio Ferreira, *Student Member, IEEE*, Shaohi Chen, James F. Antaki, and David G. Galati

Abstract—The left ventricular assist device (LVAD) is a mechanical device that can assist an ailing heart in performing its functions. The latest generation of such devices is comprised of rotary pumps which are generally much smaller, lighter, and quieter than the conventional pulsatile pumps. The rotary pumps are controlled by varying the rotor (impeller) speed. If the patient is in a health care facility, the pump speed can be adjusted manually by a trained clinician to meet the patient's blood needs. However, an important challenge facing the increased use of these LVADs is the desire to allow the patient to return home. The development of an appropriate feedback controller for the pump speed is therefore crucial to meet this challenge. In addition to being able to adapt to changes in the patient's daily activities by automatically regulating the pump speed, the controller must also be able to prevent the occurrence of excessive pumping (known as suction) which may cause collapse of the ventricle. In this paper we will discuss some theoretical and practical issues associated with the development of such a controller. As a first step, we present and validate a state-space mathematical model, based on a nonlinear equivalent circuit flow model, which represents the interaction of the pump with the left ventricle of the heart. The associated model is a six-dimensional vector of time varying nonlinear differential equations. The time variation occurs over four consecutive intervals representing the contraction, ejection, relaxation, and filling phases of the left ventricle. The pump in the model is represented by a nonlinear differential equation which relates the pump rotational speed and the pump flow to the pressure difference across the pump. Using this model, we discuss a feedback controller which adjusts the pump speed based on the slope of the minimum pump flow signal, which is one of the model state variables that can be measured. The objective of the controller is to increase the speed until the envelope of the minimum pump flow signal reaches an extreme point and maintain it afterwards. Simulation results using the model equipped with this feedback controller are presented for two different scenarios of patient activities. Performance of the controller when measurement noise is added to the pump flow signal is also investigated.

Index Terms—Cardiovascular system, left ventricular assist device (LVAD), pump speed feedback controller, rotary blood pump modeling.

I. INTRODUCTION

HEART transplantation has now been recognized as the best therapy for patients with end-stage congestive heart failure. However, potential recipients often wait long periods of time (300 days or more on the average) before a suitable donor heart becomes available, and many of these candidates, 20%–30% will die while awaiting heart transplantation. Consequently, the medical community has placed increased emphasis on the use of mechanical circulatory assist devices that can substitute for, or enhance, the function of the natural heart [1], [2]. A left ventricular assist device (LVAD) is such a device. The latest generation LVADs are built using turbo-dynamic rotary pumps, which supplement the left ventricle of the heart in meeting the circulatory demand of the patient. Generally speaking, the goal of a LVAD is to provide the patient with as close to a normal lifestyle as possible until a donor heart becomes available or, in some cases, until the patient's heart recovers. In many cases, this means allowing the patient to return home and/or to the workforce.

An important engineering challenge facing the increased use of these LVADs is the development of an appropriate controller that can adjust the speed of the rotor (pump impeller) to meet the circulatory demand of the patient [3], [4]. Such a controller, in addition to being robust and reliable, must be able to adapt to the daily activities and the physiological changes of the patient by regulating the pump speed in order to meet the body's requirements for cardiac output (CO) and mean arterial pressure (MAP). If the pump speed is too low, the blood will regurgitate from the aorta to the left ventricle through the pump resulting in what is known as "backflow." If the speed is too high, the pump will attempt to draw more blood than available which may cause a collapse of the ventricle or the flow tract to the pump resulting in a phenomenon called "suction." While avoiding these two extremes, the pump speed must also be adjusted to meet the patient's varying levels of physical activity and emotional changes [5]–[7] which are exhibited by a possibly wide variation of the patient's Systemic Vascular Resistance (SVR) [8]–[10]. The eventual goal of a pump controller is therefore to satisfy all these constraints for LVAD recipient patients to be able to leave the hospital and return home to a normal lifestyle.

Since (at this time) the technology to place sensors in the human body for long term applications does not exist, the

M. A. Simaan is with the School of Electrical Engineering and Computer Science, University of Central Florida, Orlando, FL 32826 USA (e-mail: simaan@eecs.ucf.edu).

A. Ferreira is with the Department of Electrical and Computer Engineering, University of Pittsburgh, Pittsburgh, PA 15261 USA (e-mail: alf22+@pitt.edu).

S. Chen is with the Mantaro Networks Inc., Germantown, MD 20874 USA (e-mail: shaohui.chen@gmail.com).

J. F. Antaki is with the Department of Biomedical Engineering, Carnegie Mellon University, Pittsburgh, PA 15213 USA (e-mail: antaki@andrew.cmu.edu).

D. G. Galati is with the National Robotics Engineering Consortium, The Robotics Institute, Carnegie Mellon University, Pittsburgh, PA 15201 USA (e-mail: dgalati@rec.ri.cmu.edu).
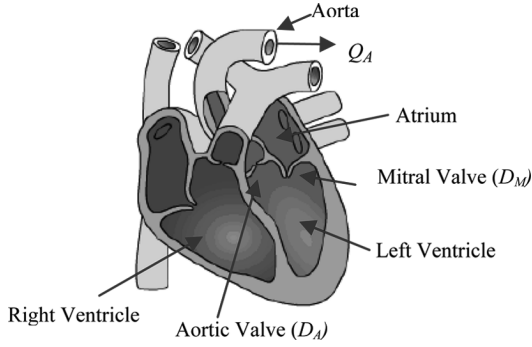
Fig. 1.   Cross section of a beating heart (http://medschool.umaryland.edu/cvrg/images/beating_heart.gif).

Fig. 2.   Cardiovascular circuit model.

TABLE I
MODEL PARAMETERS

Parameters	Value	Physiological Meaning
Resistances (mmHg.s/ml)		
R_S	1.0000	Systemic Vascular Resistance (SVR)
R_M	0.0050	Mitral Valve Resistance
R_A	0.0010	Aortic Valve Resistance
R_C	0.0398	Characteristic Resistance
Compliances (ml/mmHg)		
$C(t)$	Time-varying	Left Ventricular Compliance
C_R	4.4000	Left Atrial Compliance
C_S	1.3300	Systemic Compliance
C_A	0.0800	Aortic Compliance
Inertances (mmHg.s^2/ml)		
L_S	0.0005	Inertance of blood in Aorta
Valves		
D_M		Mitral Valve
D_A		Aortic Valve

availability of real-time measurements of the patient's hemo-dynamics for feedback control purposes is very limited. For this reason, other variables have been used for this purpose. In [11], a feedback control approach using the heart rate to control the pump speed has been reported. Although such a controller provides some advantages when compared to an open-loop fixed pump speed operation, it does not necessarily provide a mechanism to prevent the occurrence of suction. An investigation using oxygen saturation of the blood for feedback control purpose has also been reported in [12]. However this approach requires implanted transducers, and is limited in its ability to respond to sudden changes in the patient's blood demand. The use of pump flow as a feedback signal for controlling the pump speed has not yet been fully exploited. On the other hand, pump flow data can relatively easily be measured by placing a flow meter at one of the pump cannulae. In this paper, we develop a feedback controller that uses information extracted from the pump flow measurements to automatically adjust the pump speed while at the same time avoiding the occurrence of suction as much as possible.

This paper is organized as follows. In Sections II and III, a state-space model of the cardiovascular system which emphasizes the pressure-volume relationship of the left ventricle is described and validated. In Section IV, a combined cardiovascular and LVAD state-space model is presented. The model is sixth-order, nonlinear and time-varying with the rotational speed of the blood pump being the only control variable. A feedback controller for the LVAD based on the pump flow signal (one of the six state variables) is discussed in Section V. Simulation results on the performance of the controller, including tests corresponding to different scenarios of patient's activity levels (i.e., SVRs) and different signal-to-noise ratios of the measured flow signal are presented in Section VI. Concluding remarks are presented in Section VII.

II. CARDIOVASCULAR MODEL

A cross section schematic of the heart illustrating its various components is shown in Fig. 1. In order to be able to simulate the heart, numerous dynamical models of varying degree of complexity have been developed in the past ten years or so. Some of these models are represented in state space form for possible application of modern control theory. An eighth-order hybrid model of the heart which subdivides the human circ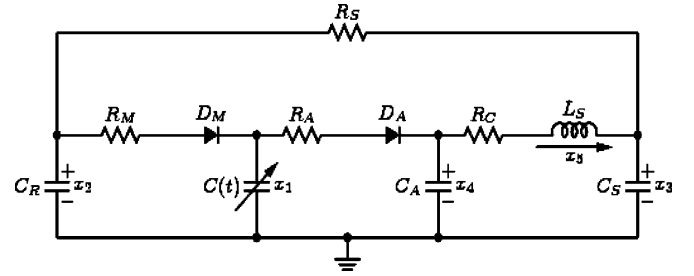ulatory system into a number of lumped parameter blocks that include the pulmonary arterial and venous systems as well as both ventricles has been developed in [13]. Although a complete heart model can be supplemented with a model for the LVAD, in this paper we assume that the right ventricle and pulmonary circulation are healthy and normal and as a result their effect on the LVAD, which is connected from the left ventricle to the ascending aorta, can be neglected [1], [6]. A fifth-order lumped parameter circuit model which can reproduce the left ventricle hemodynamics of the heart [14], [15] is shown in Fig. 2. In this model, preload and pulmonary circulations are represented by the compliance (or capacitor) C_R; the mitral valve is represented by resistor R_M and ideal diode D_M; the aortic valve is represented by resistor R_A and ideal diode D_A; the aortic compliance is represented by C_A and afterload is represented by the four-element Windkessel model comprising R_C, L_S, C_S, and R_S. In this representation, we have kept the number of model parameters at a minimum while maintaining enough complexity to reproduce the left ventricle hemodynamics. Table I lists the various system parameters and their associated values [16]–[18]. The behavior of the left ventricle is modeled by means of a time varying compliance $C(t)$, which is the reciprocal of the ventricle's elastance function $E(t)$. The elastance describes the relationship between the ventricle's pressure and volume [19] according to the expression

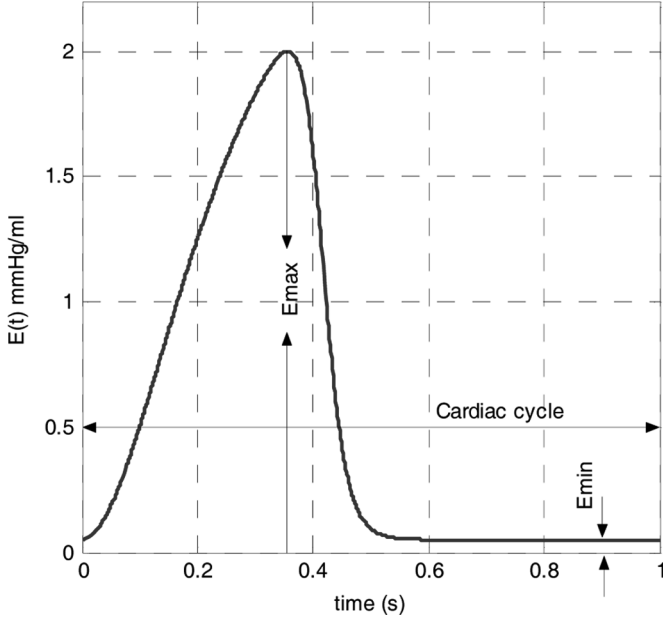$$E(t) = \frac{\text{LVP}(t)}{\text{LVV}(t) - V_0} \qquad (1)$$

Fig. 3. Elastance function of the left ventricle ($E(t) = 1/C(t)$). Cardiac Cycle $= 60/\mathrm{HR}$).

TABLE II
PHASES OF THE CARDIAC CYCLE

Modes	Valves		Phases
	Mitral	Aortic	
1	Closed	Closed	Isovolumic Relaxation
2	Open	Closed	Filling
1	Closed	Closed	Isovolumic Contraction
3	Closed	Open	Ejection
-	Open	Open	Not feasible

TABLE III
STATE VARIABLES IN CARDIOVASCULAR MODEL

Variables	Name	Physiological Meaning (units)
$x_1(t)$	LVP(t)	Left Ventricular Pressure (mmHg)
$x_2(t)$	LAP(t)	Left Atrial Pressure (mmHg)
$x_3(t)$	AP(t)	Arterial Pressure (mmHg)
$x_4(t)$	AoP(t)	Aortic Pressure (mmHg)
$x_5(t)$	$Q_T(t)$	Total flow (ml/s)

where $\mathrm{LVP}(t)$ is the left ventricular pressure, $\mathrm{LVV}(t)$ is the left ventricular volume, and V_0 is a reference volume, which corresponds to the theoretical volume in the ventricle at zero pressure. Several mathematical expressions have been derived to approximate the elastance function $E(t)$. In our work, we use

$$E(t) = (E_{\max} - E_{\min})E_n(t_n) + E_{\min} \qquad (2)$$

where $E_n(t_n)$ is the so called "double hill" function [20]

$$E_n(t_n) = 1.55 * \left[\frac{\left(\frac{t_n}{0.7}\right)^{1.9}}{1 + \left(\frac{t_n}{0.7}\right)^{1.9}} \right] * \left[\frac{1}{1 + \left(\frac{t_n}{1.17}\right)^{21.9}} \right]. \qquad (3)$$

In the above expression, $E_n(t_n)$ is the normalized elastance, $t_n = t/T_{\max}, T_{\max} = 0.2 + 0.15t_c$ and t_c is the cardiac cycle interval, i.e., $t_c = 60/\mathrm{HR}$, where HR is the heart rate. Notice that $E(t)$ is a re-scaled version of $E_n(t_n)$ and the constants $E_{\max}$ and $E_{\min}$ are related to the end-systolic pressure volume relationship (ESPVR) and the end-diastolic pressure volume relationship (EDPVR), respectively. Fig. 3 shows a plot of $E(t)$ for a normal heart with $E_{\max} = 2$ mmHg/ml, $E_{\min} = 0.06$ mmHg/ml, and a heart rate of 60 beats per minute (bpm).

Since the circuit model of Fig. 2 includes two ideal diodes D_M and D_A, four circuits representing the open-circuit (O/C) and short-circuit (S/C) states of the diodes - and hence different phases of the ventricle operation - are possible. The state in which both diodes are S/C (i.e., both the mitral and aortic valves open) is not feasible. The state in which both diodes are O/C (i.e., both the mitral and aortic valves closed) will occur twice representing the isovolumic contraction and relaxation phases of the left ventricle. When D_M is O/C and D_A is S/C the ventricle is filling, and when D_M is S/C and D_A is O/C, the ventricle is ejecting. These three different modes of operation of the left ventricle over four consecutive different time intervals within the cardiac cycle are illustrated in Table II. Clearly, every mode

operation within the cardiac cycle is modeled by a different circuit, and hence a different set of differential equations. However, by appropriately modeling the diodes as nonlinear elements, it is possible to write only one set of differential equations, which describes the behavior of the entire model for all three modes. Selecting the state variables as listed in Table III (and shown on the circuit in Fig. 2), and using basic circuit analysis methods (KVL, KCL, etc.) we can derive the state equations for the cardiovascular circuit model shown in Fig. 2 as follows:

$$\dot{x} = A_c(t)x + P_c(t)p(x) \qquad (4)$$

where $A_c(t)$ and $P_c(t)$ are 5×5 and 5×2 time-varying matrices, respectively, expressed as

$$A_c(t) = \begin{bmatrix} \frac{-\dot{C}(t)}{C(t)} & 0 & 0 & 0 & 0 \\ 0 & \frac{-1}{R_S C_R} & \frac{1}{R_S C_R} & 0 & 0 \\ 0 & \frac{1}{R_S C_S} & \frac{-1}{R_S C_S} & 0 & \frac{1}{C_S} \\ 0 & 0 & 0 & 0 & \frac{-1}{C_A} \\ 0 & 0 & \frac{-1}{L_S} & \frac{1}{L_S} & \frac{-R_C}{L_S} \end{bmatrix}$$

$$P_c(t) = \begin{bmatrix} \frac{1}{C(t)} & \frac{-1}{C(t)} \\ \frac{-1}{C_R} & 0 \\ 0 & 0 \\ 0 & \frac{1}{C_A} \\ 0 & 0 \end{bmatrix}. \qquad (5)$$

The 2×1 vector $p(x)$ in (4) models the nonlinear behavior of the diodes and is given by

$$p(x) = \begin{bmatrix} \frac{1}{R_M} r(x_2 - x_1) \\ \frac{1}{R_A} r(x_1 - x_4) \end{bmatrix} \qquad (6)$$

where $r(x)$ represents the ramp function

$$r(\xi) = \begin{cases} \xi, & \text{if } \xi \geq 0 \\ 0, & \text{if } \xi < 0. \end{cases} \qquad (7)$$

We note that the model described above is autonomous. Its solution is oscillatory in nature due to the cyclic nature of the terms
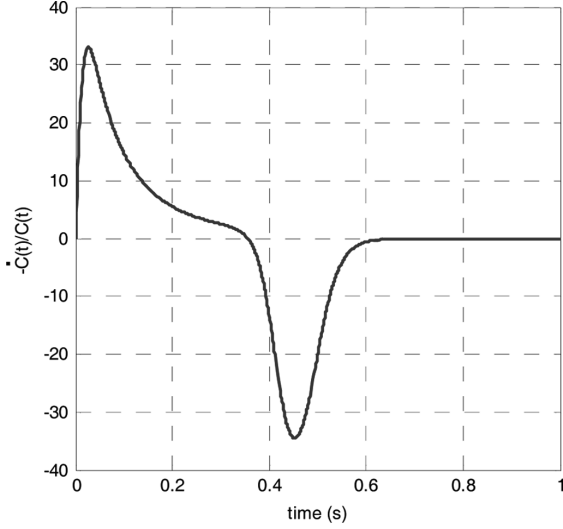
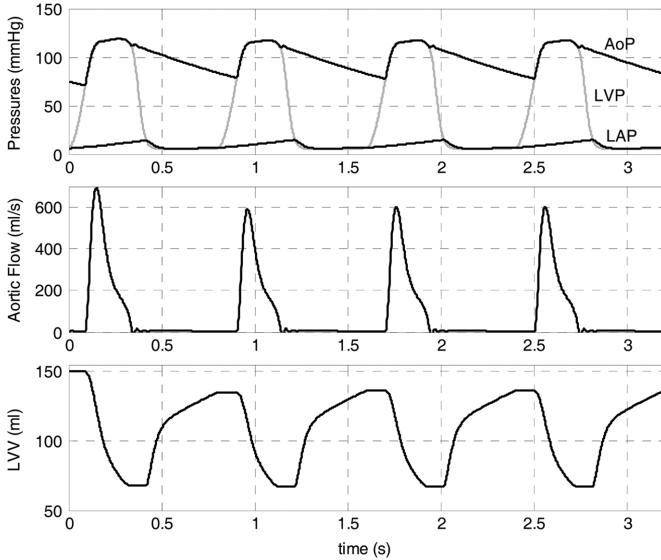Fig. 4. Plot of $-\dot{C}(t)/C(t)$ over one cardiac cycle.

Fig. 5. Simulated hemodynamic waveforms for a normal heart.

$-\dot{C}(t)/C(t)$ and $1/C(t)$ in the matrices $A_c(t)$ and $P_c(t)$ in (4). A plot of $-\dot{C}(t)/C(t)$ over one cardiac cycle is shown in Fig. 4. The term $1/C(t)$ is the elastance function $E(t)$ whose plot is shown in Fig. 3.

III. MODEL VALIDATION

The ability of the model described in the previous section to emulate the hemodynamics of the left ventricle is demonstrated by simulating the model for both nominal steady state conditions, and in response to perturbations of preload and afterload. Fig. 5 shows the simulation waveforms of the hemodynamics for an adult with heart rate of 75 bpm. In this particular case, systolic and diastolic pressure were 117 and 77 mmHg, MAP was 99 mmHg, CO was 5.21 l/min and stroke volume (SV) was 69.5 ml/beat. These numbers and waveforms are all consistent with hemodynamic data in normal subjects described in [21].

Another way to validate the model and verify that it can reproduce the human left ventricle behavior is to vary the preload and afterload conditions, while keeping the left ventricle parameters (E_{max}, E_{min}, and V_0) constant. If the model behaves as expected, we should have an approximately linear relationship between end-systolic pressure and left ventricle volume (known as ESPVR), in spite of changes in preload and afterload. A total of four preload and four afterload conditions were simulated. In these tests, we set $E_{max} = 2$ mmHg/ml, $E_{min} = 0.05$ mmHg/ml, and $V_0 = 10$ ml. The resulting pressure and volume of the ventricle are typically plotted in the form of PV-loops. The PV-loops in Fig. 6(a), represent the result of changing afterload conditions by selecting different values of Systemic Vascular Resistance (R_S in Fig. 2), while keeping end diastolic volume (EDV) constant. The PV-loops in Fig. 6(b) represent the result of altering preload conditions by changing the Mitral valve resistance R_M. The linear relationship between pressure and volume is evident in both Figs. 6(a) and (b). The slope of the ESPVR and the horizontal intercept for the afterload data in Fig. 6(a) are determined as 1.98 mmHg/ml and 10.91 ml, respectively. For the preload data of Fig. 6(b) these values are determined as 1.92 mmHg/ml and 8.84 ml, respectively. These results are consistent with the values used for E_{max} and V_0 used in the simulation and clearly show that the cardiovascular model can indeed mimic the behavior of the left ventricle.

A third way to validate the model is to compare the hemodynamic waveforms obtained from the model to those of a human patient. Fig. 7 shows left ventricular pressure data and the corresponding PV-loop obtained from our model using values $E_{max} = 1.5$ mmHg/ml and $V_0 = 12$ ml estimated from real data of a patient suffering from cardiomyopathy. The measured data from the patient are also superimposed on the same plots in Fig. 7. Clearly the data from the model represents a close fit to the real measured patient data. As a test for how close the two data sets match, in the case of LVP, the error was calculated to be 4.4% and in the case of the PV-loop, the area within the loop known as the stroke work (SW) was determined to be 10 492 mmHg.ml for the PV-loop of the model and 10 690 mmHg.ml for the patient PV-loop which represents a difference of 1.85%.

IV. CARDIOVASCULAR-LVAD MODEL

The LVAD considered in this paper is a rotary blood pump connected as a bridge between the left ventricle and the aorta as illustrated in the schematic in Fig. 8. A model of the pump (LVAD, Nimbus Inc, Rancho Cordova, CA, [22]) connected to the cardiovascular model of Fig. 2 is shown in Fig. 9. The addition of the LVAD circuit to the network adds one state variable and five passive parameters. The state variable $x_6(t)$ represents the blood flow through the pump. Resistors R_i and R_o and inductors L_i and L_o represent the inlet and outlet resistances and inertances, respectively, of the pump cannulae. The fifth parameter R_k is a time varying, nonlinear, pressure-dependent resistor which simulates the phenomenon of suction [5], [23]. It is represented by the expression

$$R_k = \begin{cases} 0, & \text{if } x_1(t) > \bar{x}_1 \\ \alpha(x_1(t) - \bar{x}_1), & \text{if } x_1(t) \leq \bar{x}_1 \end{cases} \quad (8)$$
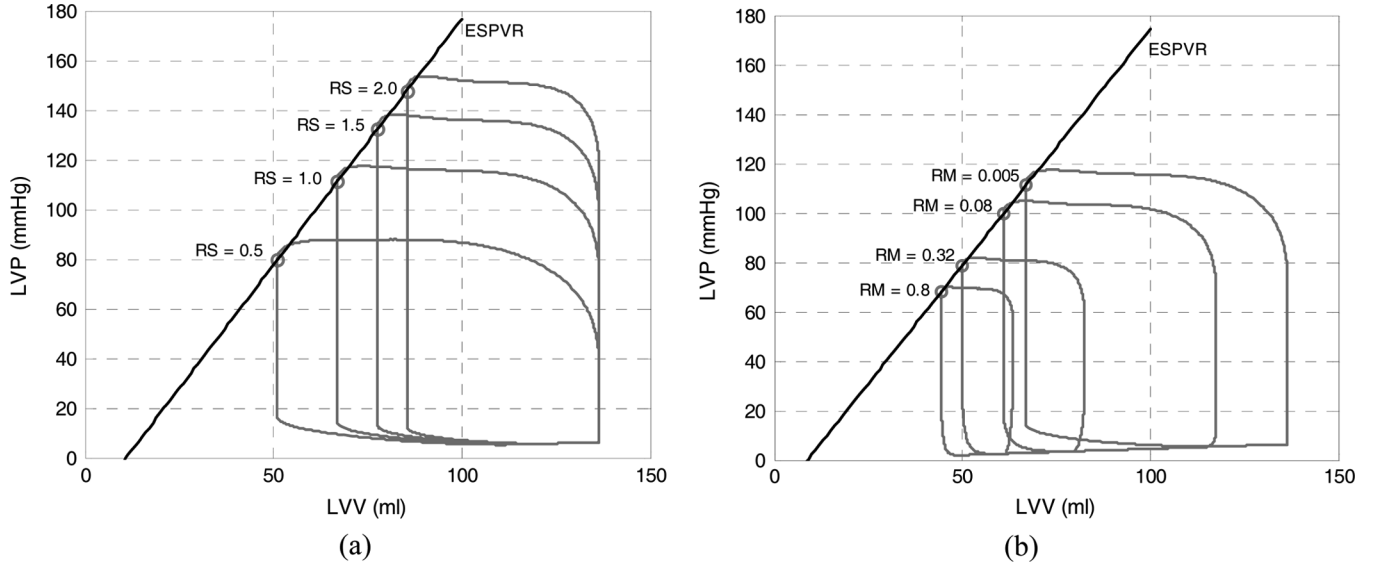
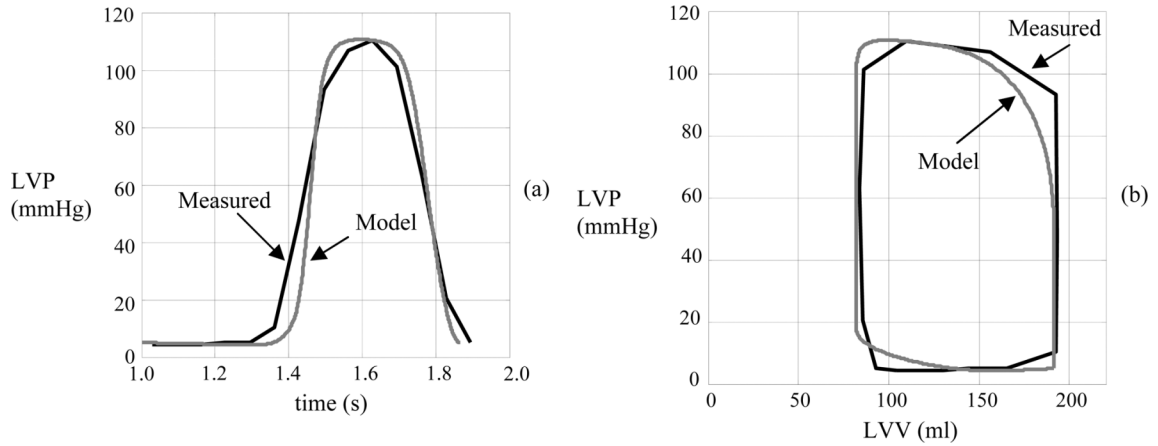Fig. 6. PV loops for different values of (a) afterload resistance and (b) preload volume.

Fig. 7. Measured and simulated (a) left ventricular pressure and (b) PV-loops.
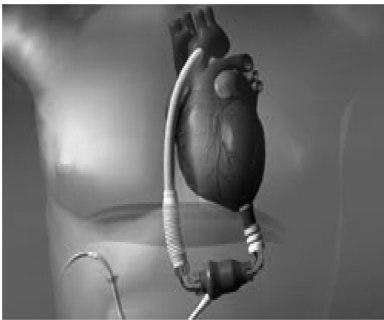

Fig. 8. Schematic of a rotary LVAD connected between the left ventricle and the arota (http://www.tmc.edu/thi/thoratec_heartmateii.html).

where α and $\bar{x}_1$ are LVAD-dependent weight parameter and threshold pressure, respectively. Finally, in the circuit of Fig. 9,

H represents the pressure difference (inlet-outlet) across the pump and is defined by the following characteristic equation [22] in terms of the pump flow x_6 and pump speed ω

$$H = \beta_0 x_6 + \beta_1 \frac{dx_6}{dt} + \beta_2 \omega^2 \qquad (9)$$

where β_0, β_1, and β_2 are also LVAD-dependent parameters. Values of all parameters mentioned above for the specific LVAD used in our model are given in Table IV.

Note that the combined cardiovascular and LVAD model is now a forced system, where the primary control variable is the pump speed ω. As was done for the cardiovascular model, the state equations for this combined sixth-order model can be derived from basic circuit analysis techniques and written in the form

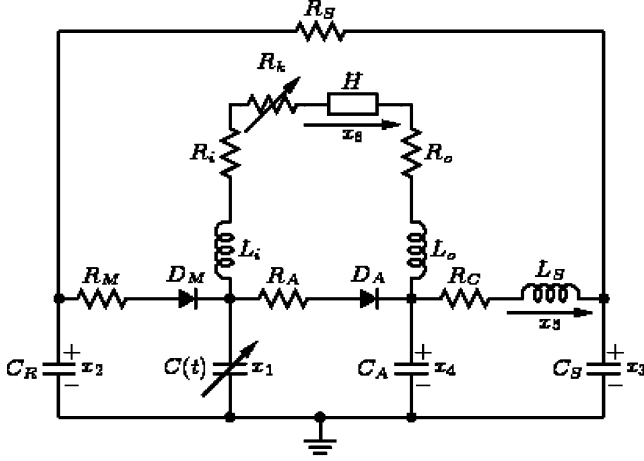$$\dot{x} = A(t)x + P(t)p(x) + bu(t) \qquad (10)$$

Fig. 9. Combined cardiovascular and LVAD model.

TABLE IV
MODEL PARAMETERS FOR THE LVAD

Parameters	Value	Physiological Meaning
Cannulae Resistances (mmHg.s/ml)		
R_i	0.0677	Inlet Resistance of Cannulae
R_o	0.0677	Outlet Resistance of Cannulae
R_k	See (8)	Suction Resistance with parameters: $\alpha = -3.5$ s/ml and $\bar{x}_1 = 1$ mmHg.
Cannulae Inertances (mmHg.s²/ml)		
L_i	0.0127	Inlet Inertance of Cannulae
L_o	0.0127	Outlet Inertance of Cannulae
Pressure Difference Parameters		
β_0	-0.17070	
β_1	-0.02177	
β_2	$9.9025 * 10^{-7}$	

where $A(t)$ and $P(t)$ are 6×6 and 6×2 time-varying matrices and b is a 6×1 constant matrix, respectively, given by the expressions

$$A(t) = \begin{bmatrix} \frac{-\dot{C}(t)}{C(t)} & 0 & 0 & 0 & 0 & \frac{-1}{C(t)} \\ 0 & \frac{-1}{R_S C_R} & \frac{1}{R_S C_R} & 0 & 0 & 0 \\ 0 & \frac{1}{R_S C_S} & \frac{-1}{R_S C_S} & 0 & \frac{1}{C_S} & 0 \\ 0 & 0 & 0 & 0 & \frac{-1}{C_A} & \frac{1}{C_A} \\ 0 & 0 & \frac{-1}{L_S} & \frac{1}{L_S} & \frac{-R_C}{C_S} & 0 \\ \frac{1}{L^*} & 0 & 0 & \frac{-1}{L^*} & 0 & \frac{-R^*}{L^*} \end{bmatrix}$$

$$P(t) = \begin{bmatrix} \frac{1}{C(t)} & \frac{-1}{C(t)} \\ \frac{-1}{C_R} & 0 \\ 0 & 0 \\ 0 & \frac{1}{C_A} \\ 0 & 0 \\ 0 & 0 \end{bmatrix}$$

$$b = \begin{bmatrix} 0 \\ 0 \\ 0 \\ 0 \\ 0 \\ \frac{-\beta_2}{L^*} \end{bmatrix} \quad (11)$$

and $p(x)$ is a 2×1 vector, given in (6), which models the nonlinear behavior of the diodes. In (11), the elements L^* and R^* are given by the expressions

$$L^* = L_i + L_o + \beta_1 \quad (12)$$
$$R^* = R_i + R_o + R_k + \beta_o. \quad (13)$$

The control variable in (10) is $u(t) = \omega^2(t)$, where $\omega(t)$ is the rotational speed of the pump.

V. DEVELOPMENT OF A FEEDBACK CONTROLLER

The only available mechanism to control a rotary LVAD is to increase or decrease the speed of rotation of the pump in order to meet certain goals typically related to the well being of the patient [3]. For a patient whose level of activity is continuously changing, one important objective of a controller for the LVAD is to vary the speed in such a way that the patient is provided with the required cardiac output while at the same time insuring that suction does not occur by unnecessary, excessive pumping. The achievement of these two goals has been a major challenge for LVAD developers for over 15 years and is recognized as one of the most serious limitations of this technology at this time. A manual open-loop controller will not be able to achieve the above objectives without an ability to observe the pump flow (visually) or cardiac chambers (for example, by echocardiography) and adjust the speed accordingly. A full state feedback controller, on the other hand, may be developed if the hemodynamic variables (x_1 through x_5) can be continuously measured in real-time. However, current implantable sensor technology to achieve this goal does not exist. The pump flow state variable x_6, on the other hand, is the only state variable that can be measured in real time. This can be done, for example, by using standard ultrasonic flow transducers that can be clamped on one of the pump cannulae.

A plot of a pump flow signal measured in an animal in-vivo study[1] in which the WorldHeart[2] LVAD was used is shown in Fig. 10. In this study the pump speed is increased linearly until suction is reached while observing the pump flow signal. This data shows that the onset of suction is characterized by several phenomena which includ: 1) a sudden large drop in the slope of the envelope of the minimum pump flow signal and 2) a sudden change in the signature of the pump flow signal. While any of these two characteristics may be used in the development of a speed controller; in this paper, we will present results related to using the slope of the minimum pump flow signal as the primary feedback variable for controlling the pump speed. The use of time-frequency characteristics of the various patterns in the pump flow signal to control the pump is currently under investigation and some preliminary results have been reported in [24] and [25].

It is clear from Fig. 10 that the slope of the envelope of the minimum pump flow signal is generally positive in the safe zone prior to the onset of suction and abruptly changes sign to a large negative value when suction occurs. This can also be clearly seen on Fig. 11 which shows a plot of the envelope of the minimum

[1]Authorized according to WorldHeart, Inc. IRB DO 01-06002.

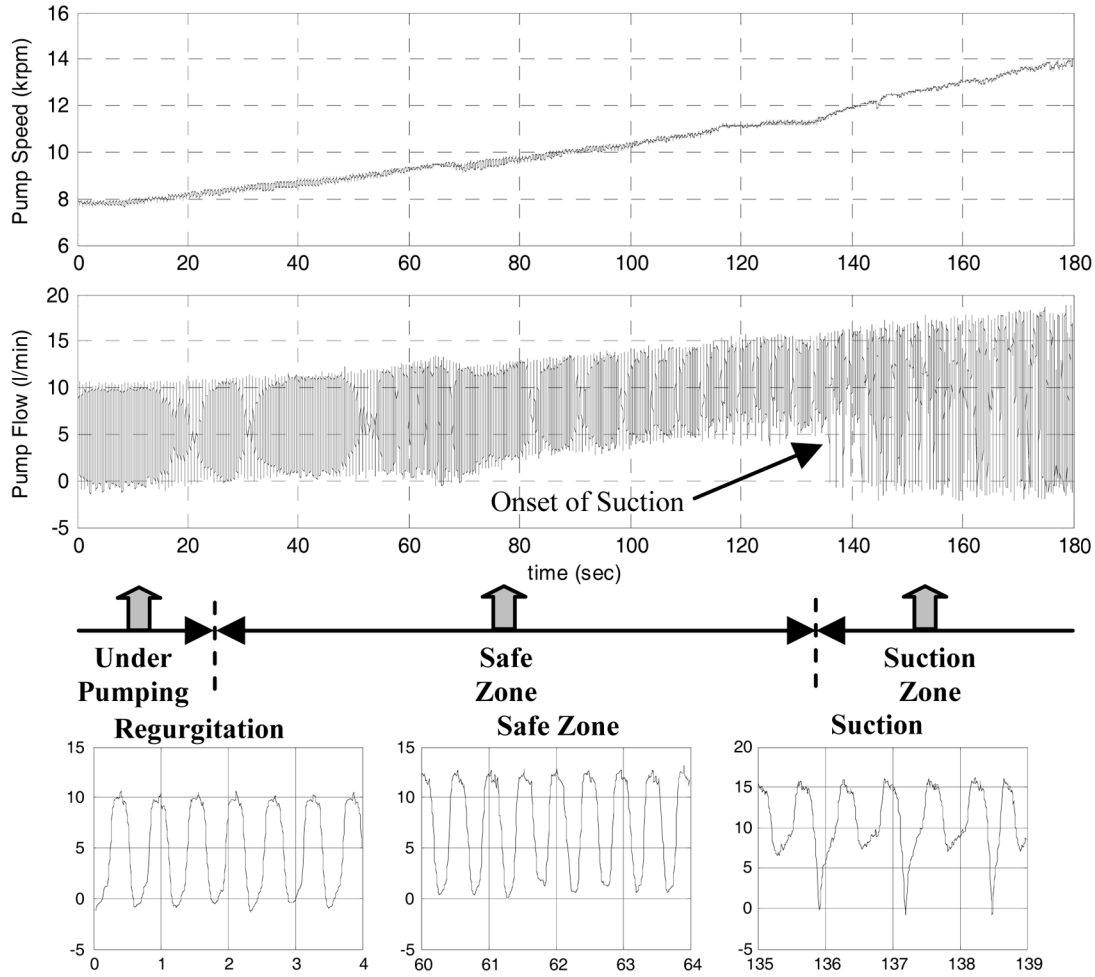[2]WorldHeart, Inc., formerly MedQuest, Inc., Salt Lake City, UT.

Fig. 10. *Invivo* pump flow data as pump speed is increased obtained from animal implanted with rotary blood pump.
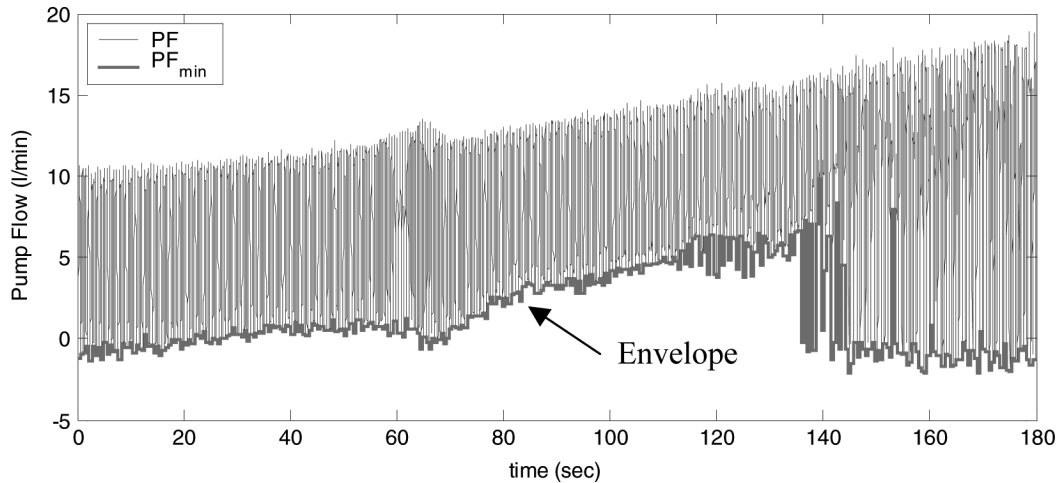

Fig. 11. Envelope of the *in-vivo* minimum pump flow signal shown in Fig. 10.

pump flow signal of Fig. 10. In this plot the values of pump flow within each cardiac cycle are replaced by the minimum value within that cycle. Many clinicians assume that the onset of suction occurs when the slope of the minimum pump flow envelope is near zero, changing from a positive value to a large negative value (this occurs at ~11 500 r/min in Figs. 10 or 11).

Since the pump flow signal is one of the state variables (x_6) in our model, the first step is to examine the behavior of this variable when our model is excited by a linearly increasing pump speed. Fig. 12 shows the pump flow signal x_6 when the model is excited by a pump speed ω which increases linearly from 12 000 to 18 000 r/min over a 60-s time period. Clearly, the resulting
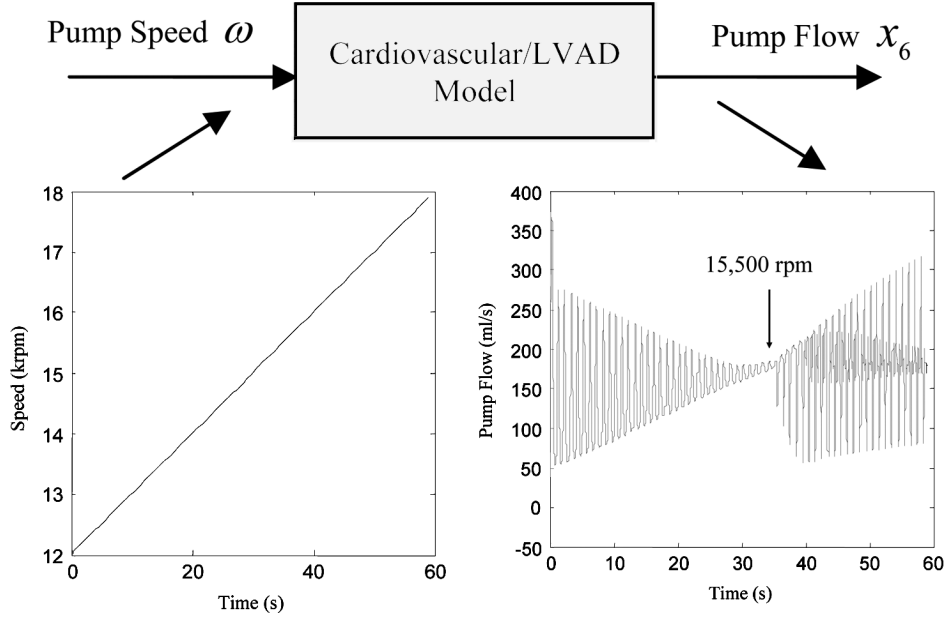
Fig. 12.   Pump flow signal from human cardiovascular/LVAD model as a function of linearly increasing pump speed. Suction occurs at 15 500 r/min.
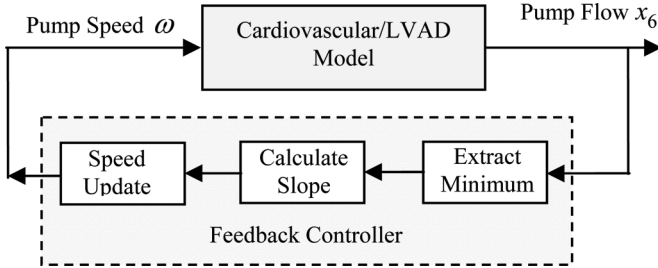

Fig. 13.   Pump speed feedback controller.

pump flow signal has similar characteristics as the in-vivo animal data in that the slope of the envelope of the minimum pump flow changes sign from positive to a large negative value at the onset of suction (which occurs when ω reaches 15 500 r/min in Fig. 12).

A general block diagram of our feedback controller is illustrated in Fig. 13. The controller consists of two basic functions. The first, labeled "Extract Minimum" will track the minimum value of the pump flow signal within each cardiac cycle. Clearly the locations of these minima are synchronized among all cardiac cycles. The second, labeled "Calculate Slope," will estimate the slope of the envelope of minimum values. This slope is estimated by fitting, in a least-squares sense, a straight line to a moving window consisting of past minimum values of the pump flow signal. A window consisting of a large number of past values is effective in noisy pump flow data because of the noise filtering effect of the least-squares fitting method. For data where the noise is negligible, a short window consisting of a small number of past values will provide the best estimate of the slope. The slope of the straight line is computed and denoted as $d\underline{x}_6/dt$, where $\underline{x}_6$ denotes the envelope of the minimum pump flow signal x_6. The third function, labeled "Speed Update" provides a mechanism for adjusting the pump speed based on the

calculated slope until the maximum of the minimum pump flow signal is reached. The update rule that we use is as follows:

$$\omega(k+1) = \omega(k) + c \left. \frac{d\underline{x}_6}{dt} \right|_{t=k*\Delta t} \tag{14}$$

where k is the update sample, $\Delta t = 0.005$ s and c is a constant gain parameter which controls the rate of speed adjustment (note that c should be less than the slew rate of the pump speed). Depending on the patient, a small value of c will result in a slow adjustment process, while a large value of c will increase the rate of adjustment at the risk of overshoot and driving the pump into suction. We should note that the size of the window in estimating the slope and the value of c in the speed update mechanism are typically chosen by a clinician and may vary depending on quality of the pump flow data and the condition of the patient. Initially, the pump speed is started below suction when $d\underline{x}_6/dt > 0$ and then increased according to (14) until $d\underline{x}_6/dt$ becomes close to zero, at which point it will be maintained below the suction speed.

VI. SIMULATION RESULTS

As mentioned earlier, the main objective of the controller is to adjust the pump speed so that it remains below the level at which suction occurs. The suction speed, however, varies depending on the level of activity of the patient which we model in terms of the SVR R_S. Thus, in order to be able to assess the performance of our controller we need to determine (i.e., know a priori) the suction speed as a function of R_S. This can be achieved by exciting the cardiovascular/LVAD model with an open-loop ramp speed control, as shown in Fig. 12. The resulting pump flow signals for five different values of R_S are shown in Fig. 14(b)–(f). A plot of the suction speed vs R_S is shown in Fig. 15. To assess the performance of the controller, we performed the following three simulations. In all of these simulations, the slope estimation was done using a window of 2.5 sec which includes three
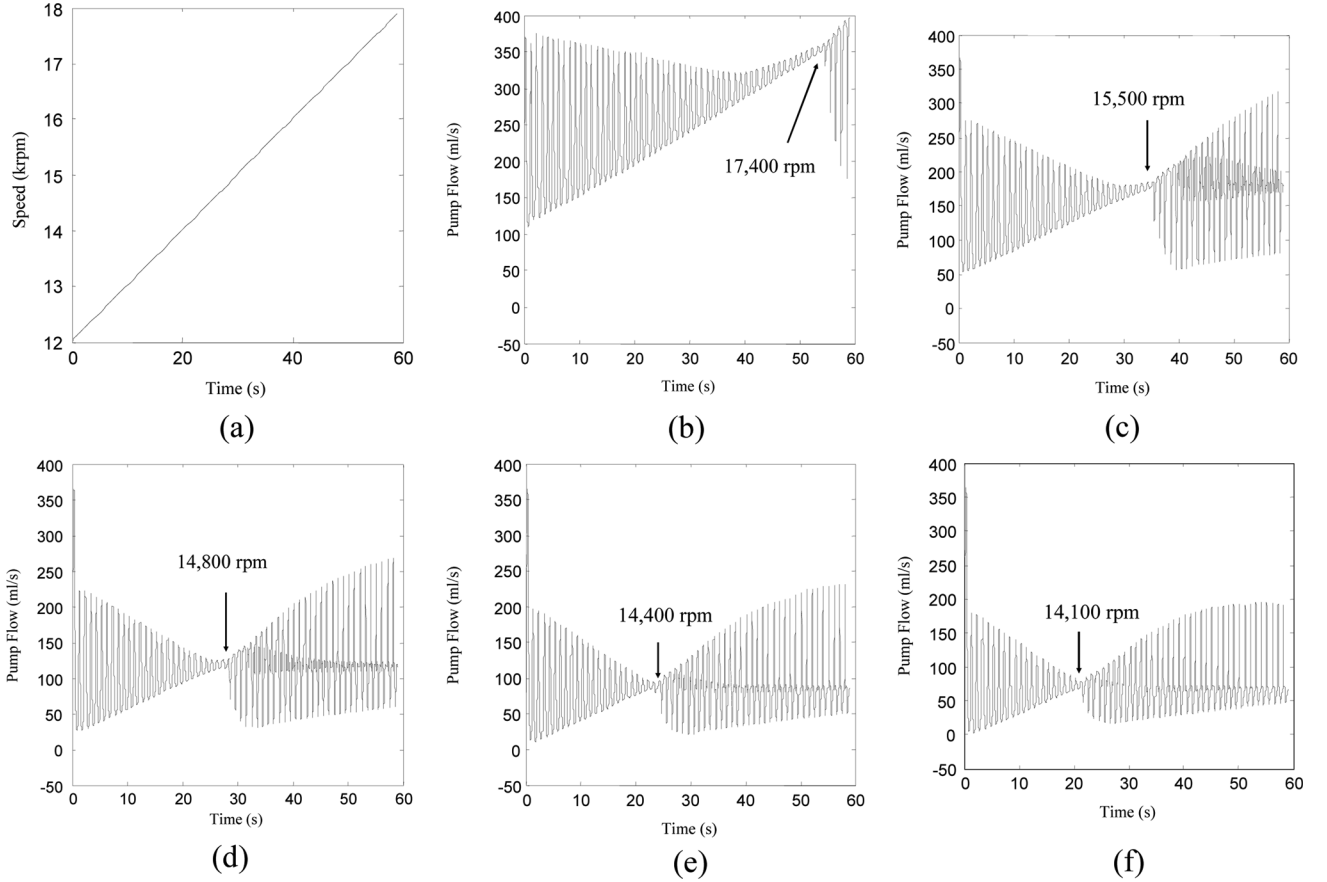
Fig. 14. (a) Ramp speed and pump flow signals for (b)–(f) different values of SVR. (a) Ramp speed profile, (b) $R_s = 0.5$, (c) $R_s = 1.0$, (d) $R_s = 1.5$, (e) $R_s = 2.0$, (f) $R_s = 2.5$.
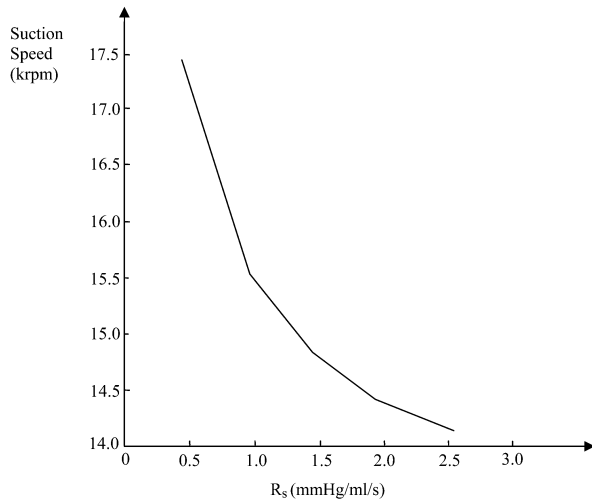

Fig. 15. Suction speed as a function of systemic resistance.

minimum pump flow values (the point in question plus the two immediate past minimum pump flow values). A value of c equal to 0.76 rpm/(ml/s) was used in the speed adjustment mechanism.

Simulation 1: Constant Systemic Vascular Resistance: Constant SVR typically represents a patient whose level of activity remains unchanged for a period of time. In this simulation, we set the SVR at $R_S = 1.0$ mmHg/ml/s for which the suction

speed as indicated from Fig. 14 is $\omega_s = 15\,500$ r/min. Fig. 16(a) shows a plot of pump speed versus time as generated by our feedback controller and Fig. 16(b) shows a plot of the corresponding pump flow signal versus time. Clearly, these figures indicate that the controller was able to increase and maintain the pump speed to a level below the suction speed. A comparison of this controller's performance with a controller based on maintaining the pressure Δp between the left heart and the aorta close to a reference pressure $\Delta p_r = 75$ mmHg, [3], [26], [27] for different values of SVR is given in Table V. In this comparison, the Δp method was implemented with a speed update gain of 0.004 rad/s/mmHg and a step size is 0.005 s. Clearly, these two controllers based on two completely different objectives, performed slightly differently, but both gave acceptable results. In all cases the Cardiac Output and Mean Arterial Pressures are slightly higher with the minimum pump flow controller, due to the higher pump speed that resulted with this controller.

Simulation 2: Changing Systemic Vascular Resistance: In order to simulate a situation representing a patient with a changing level of activity, we kept the value of SVR at 1.0 mmHg/ml/s for one half of the time duration and increased it to 2.0 mmHg/ml/s for the remaining duration of the test. That is

$$R_S = \begin{cases} 1, & \text{for } 0 \leq t \leq 27.5 \\ 1 + (t - 27.5)/5, & \text{for } 27.5 < t \leq 32.5 \\ 2, & \text{for } 32.5 < t \leq 60. \end{cases} \quad (15)$$
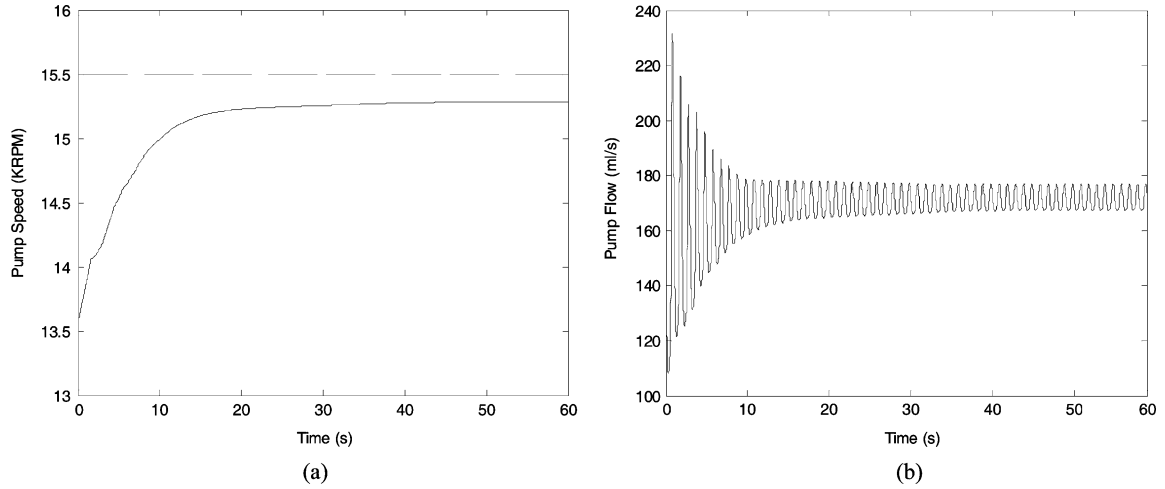
Fig. 16. (a) Pump speed (solid line) generated by the feedback controller. Suction speed (dashed line). (b) Pump flow generated by the feedback controller (simulation 1).
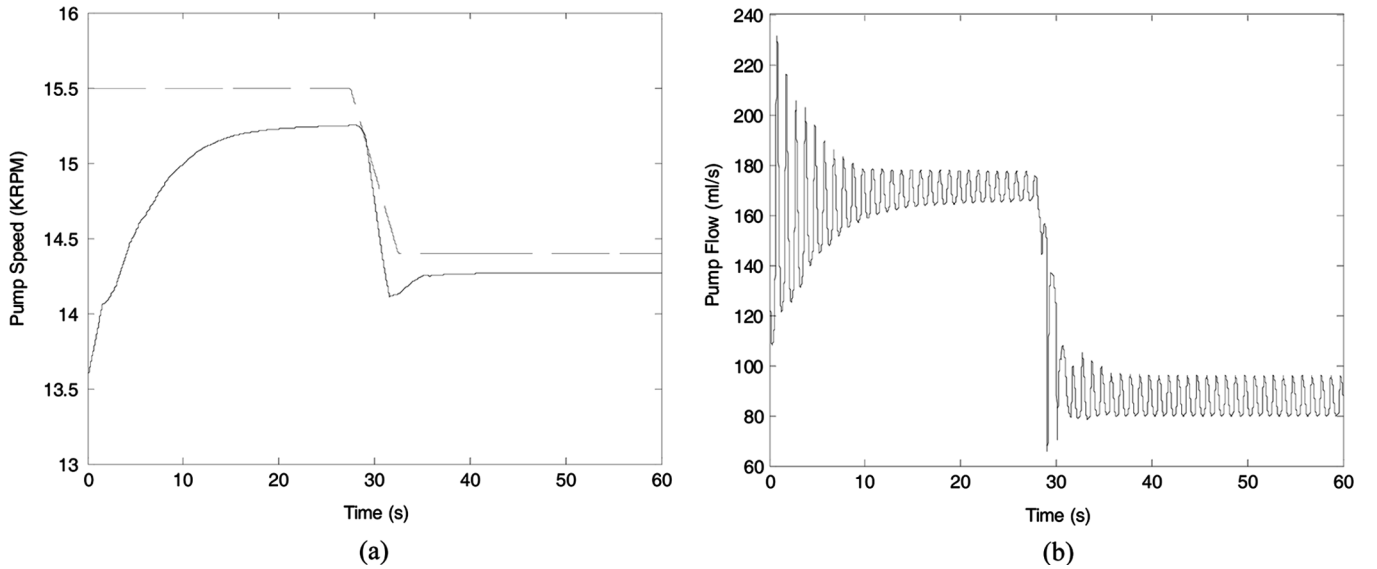

Fig. 17. (a) Pump speed (solid line) generated by the feedback controller. Suction speed (dashed line). (b) Pump flow generated by the feedback controller (simulation 2).

TABLE V
COMPARISON OF MINIMUM PUMP FLOW AND CONSTANT Δp METHODS
(WITH $\Delta p_r = 75$)

		Cardiac Output (L/min)	Mean Arterial Pressure (mmHg)
SVR=0.5	Min. Pump Flow	14.4	136
	Constant Δp	11.7	110
SVR=1.0	Min. Pump Flow	7.5	133
	Constant Δp	6.5	120
SVR=2.0	Min. Pump Flow	3.8	132
	Constant Δp	3.7	137

The increase in R_S can be viewed as representing a drop in level of activity of the patient (i.e., a patient who was walking for some time and then rested by returning to his/her bed). The rapid change in the patient's activity level over a period of 5 s

represents a worse case scenario than what actually happens to people in real life. The suction speeds for these two values of SVR (see Fig. 14) are 15 500 and 14 400 r/min, respectively. The response of our feedback controller in adjusting the pump speed is shown in Fig. 17(a) and the resulting pump flow signal is shown in Fig. 17(b). Here again, clearly the speed was properly adjusted up and then down to meet the patient blood flow demand while at the same time it did not exceed the suction level for the entire duration of the simulation.

Simulation 3: Constant and Changing Systemic Vascular Resistance With Noisy Pump Flow Measurements: Since our feedback controller relies mainly on one state variable (the pump flow signal), it important to assess its performance when measurement noise is present. To do this, we repeated the previous two simulations with uniformly distributed random noise added to the pump flow measurement. Figs. 18 and 19 show the results for two different noise levels (corresponding to SNR =
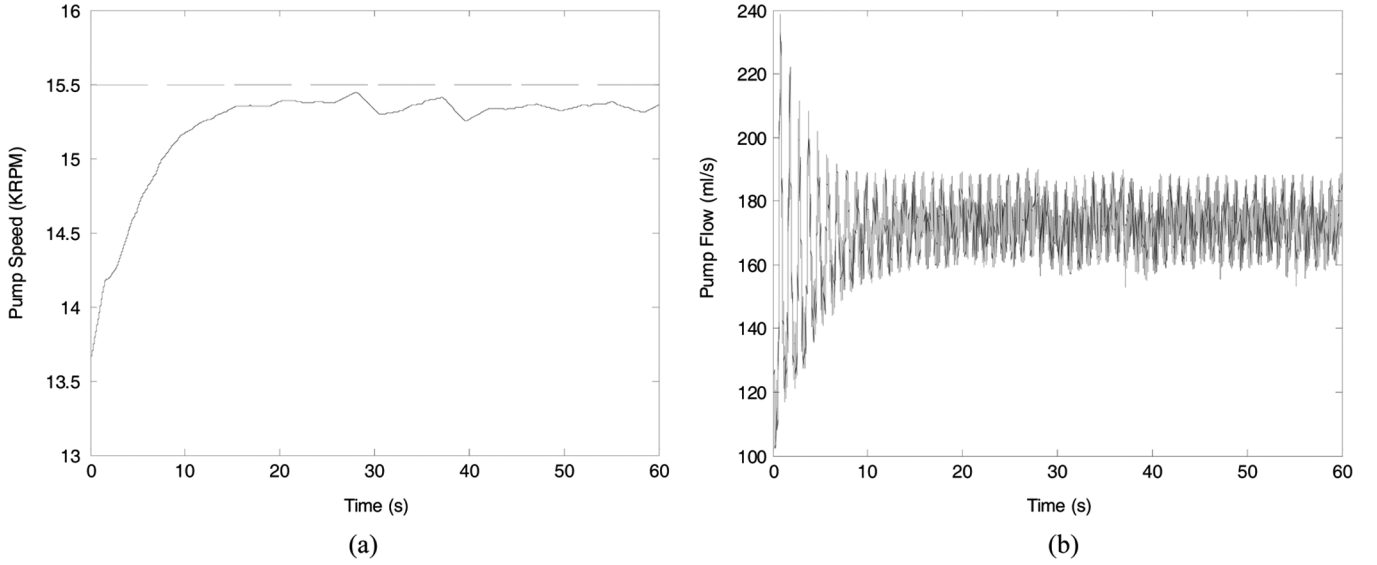
Fig. 18. (a) Pump speed (solid line) generated by the feedback controller. Suction speed (dashed line). (b) Pump flow generated by the feedback controller [simulation 1 with $\mathrm{SNR} = 29.48$ dB)].
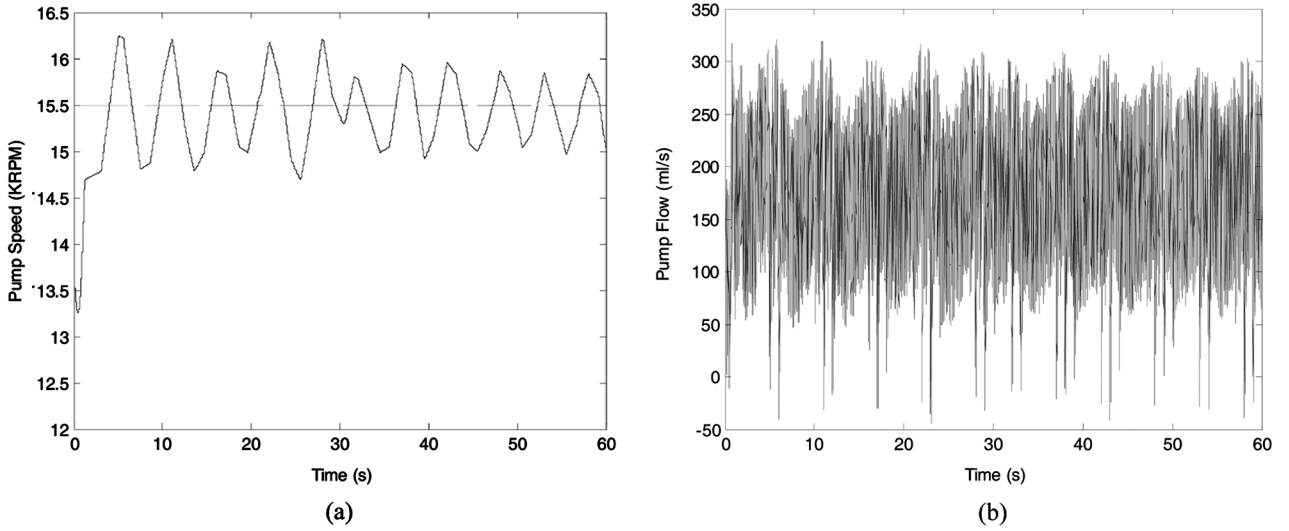

Fig. 19. (a) Pump speed (solid line) generated by the feedback controller. Suction speed (dashed line). (b) Pump flow generated by the feedback controller [simulation 1 with $\mathrm{SNR} = 6.28$ dB)].

29.48 dB and $\mathrm{SNR} = 6.28$ dB, respectively) in the pump flow measurements of Simulation 1, and Figs. 20 and 21 show the results for two different noise levels (corresponding to $\mathrm{SNR} = 29.40$ dB and $\mathrm{SNR} = 5.48$ dB, respectively) in the pump flow measurements of Simulation 2. Clearly, in both simulations, while the controller performed very well by keeping the pump speed below the suction speed for a high SNR, it did not do as well when the SNR decreased to lower values. In the latter case, because of the high level of noise in the pump flow signal [as is clear in Figs. 19(b) and 21(b)], the pump speed was getting in and out of suction frequently during the 60-s duration of the simulation. Two indexes have been developed to assess how well the controller performed as a function of SNR in the pump flow measurements: The first index ρ is defined as the percentage of

the total time during which the actual pump speed has exceeded the suction speed, as illustrated in Fig. 22. That is

$$\rho = \frac{\sum_{i=1}^{i=I} \Delta t_i}{T} \times 100 \tag{15}$$

where Δt_i is the ith interval over which the actual pump speed exceeded the suction speed, and I is the number of such intervals.

The second index η is a measure of how deep, on the average, the pump speed penetrates into the suction region. This index is quite important since a pump speed slightly in excess of the suction speed over a short period of time can often be tolerated by the patient. It is calculated as follows. First, the average speed
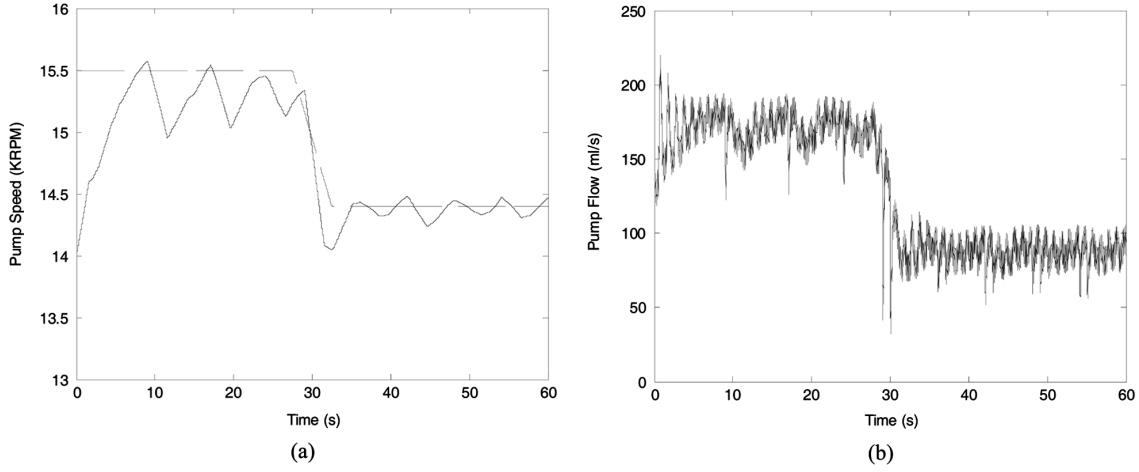
Fig. 20. (a) Pump speed (solid line) generated by the feedback controller. Suction speed (dashed line). (b) Pump flow generated by the feedback controller [simulation 2 with $\mathrm{SNR} = 29.40$ dB)].
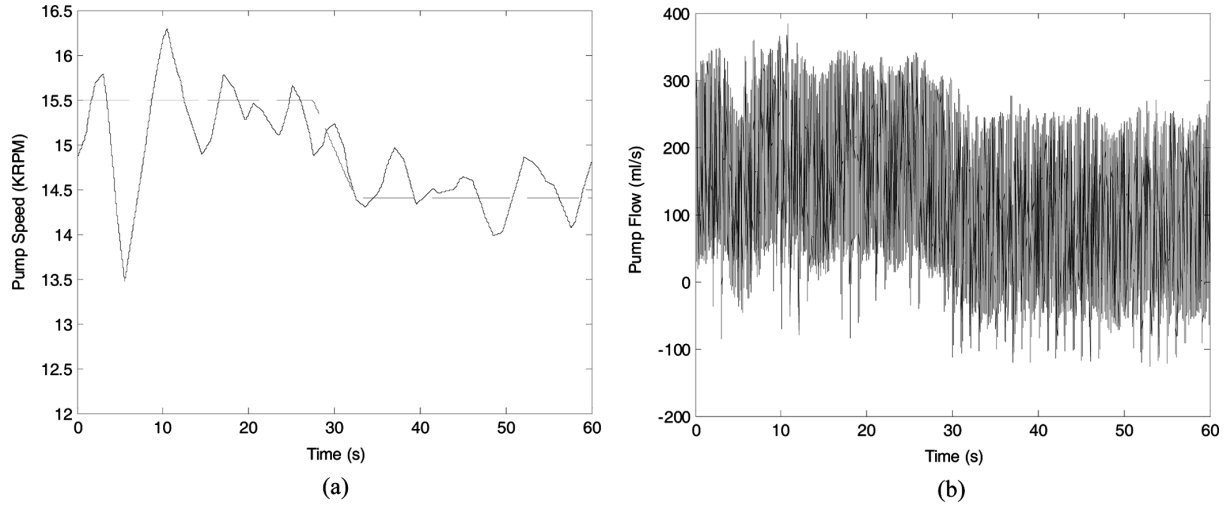

Fig. 21. (a) Pump speed (solid line) generated by the feedback controller. Suction speed (dashed line). (b) Pump flow generated by the feedback controller [simulation 2 with $\mathrm{SNR} = 5.48$ dB)].
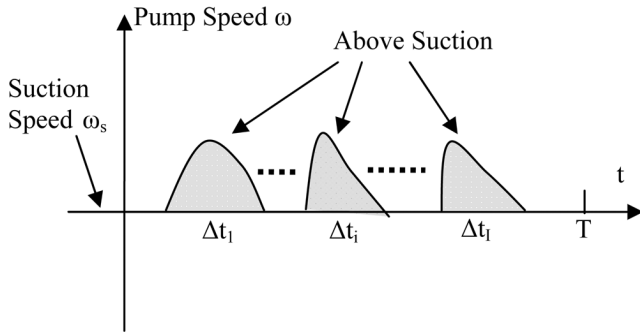

Fig. 22. Intervals of time Δt_i during which the pump speed exceeds the suction speed.

TABLE VI
PERFORMANCE INDEXES VERSUS SNR

Pump Flow SNR (dB)	ρ %	η %
29.48	0.00	0.00
25.85	0.00	0.00
19.90	6.69	0.15
14.92	15.94	0.72
10.47	23.72	1.34
6.28	40.33	1.90

$\overline{\omega_s}$ over the intervals when the pump speed exceeded the suction speed is computed as follows:

$$\overline{\omega_s} = \frac{\sum_{i=1}^{i=I} \int_{\Delta t_i} \omega(t) dt}{\sum_{i=1}^{i=I} \Delta t_i}. \qquad (16)$$

Then the average percent pump speed penetration into suction is calculated according to the expression

$$\eta = \frac{\overline{\omega_s} - \omega_s}{\omega_s} \times 100 \qquad (17)$$

where ω_s is the suction speed. Both of these performance indexes were calculated for six different levels of SNR in Simulation 1 (constant SVR). The results are shown in Table VI. Clearly, as expected, both of these indexes increased as the SNR decreased

from 29.48 dB to 6.28 dB. In the worst possible SNR case, however, the pump speed exceeded the suction speed on the average by 1.9% (i.e., $\sim$ 300 r/min over the suction speed of 15 500 r/min) for 40.33% of the time it was in operation. While at this time there are no clinical studies that would indicate whether this level of penetration is acceptable or not, all indications is that the patient might experience some discomfort due the intermittent low level of suction that would occur at this SNR.

VII. CONCLUSION

In this paper, we presented a comprehensive state-space model for a LVAD connected to the cardiovascular system. The model is a sixth-order, highly nonlinear set of differential equations operating over four different time regions within one cardiac cycle. Using this model, we developed a patient adaptive feedback controller for the pump speed in the LVAD which insures that the patient's blood flow requirements are met as a function of the patient's activity level and at the same time avoid the occurrence of suction. Because of the fact that five out of the six state variables cannot be measured using current sensor technology, we developed our feedback controller based on one state variable (the pump flow signal) which is considered available for measurements. Several simulations were performed to test the performance of our controller under varying patient activity levels and signal to noise ratios of the pump flow measurements. Our results show that for moderate to high signal to noise ratios, the controller performed extremely well in adjusting the speed and keeping it below suction at all time. However, in cases with low signal to noise ratios the controller could not avoid suction entirely, but its performance would still be considered within the acceptable range. In the worst possible case of $\mathrm{SNR} = 6.28$ dB, the controller intermittently exceeded the suction speed only by 1.9% on the average (i.e., $\sim$ 300 r/min) for about 40% of the time it was in operation.

REFERENCES

[1] V. L. Poirier, "The LVAD: A case study," *The Bridge*, vol. 27, pp. 14–20, 1997.

[2] H. Frazier and T. J. Myers, "Left ventricular assist systems as a bridge to myocardial recovery," *Annals Thoracic Surg.*, vol. 68, pp. 734–741, 1999.

[3] D. B. Olsen, "The History of Continuous-Flow Blood Pumps," *Artif. Organs*, vol. 24, no. 6, pp. 401–404, 2000.

[4] J. R. Boston, J. F. Antaki, and M. Simaan, "Hierarchical control for hearts assist devices," *IEEE Robot. Autom. Mag.*, vol. 10, no. 1, pp. 54–64, Mar. 2003.

[5] H. Shima, W. Trubel, A. Moritz, G. Wieselthaler, H. G. Stohr, H. Thomas, U. Losert, and E. Wolner, "Noninvasive monitoring of rotary blood pumps: Necessity, possibilities, and limitations," *Artif. Organs*, vol. 14, no. 2, pp. 195–202, 1992.

[6] H. Konishi, J. F. Antaki, and D. V. Amin, "Controller for an axial flow blood pump," *Artif. Organs*, vol. 20, no. 6, pp. 618–620, 1996.

[7] Y. Wu, P. Allaire, G. Tao, H. Wood, D. Olsen, and C. Tribble, "An advanced physiological controller design for a left ventricular assist device to prevent left ventricular collapse," *Artif. Organs*, vol. 27, no. 10, pp. 926–930, 2003.

[8] G. Giridharan, G. Pantalos, S. Koenig, K. Gillars, and M. Skliar, "Achieving physiologic perfusion with ventricular assist devices: Comparison of control strategies," in *Proc. 2005 Amer. Contr. Conf.*, Portland, OR, Jun. 8–10, 2005, pp. 3823–3828.

[9] S. Chen, J. F. Antaki, M. A. Simaan, and J. R. Boston, "Physiological control of left ventricular assist devices based on gradient of flow," in *Proc. 2005 Amer. Contr. Conf.*, Portland, OR, Jun. 8–10, 2005, pp. 3829–3834.

[10] K.-W. Gwak, M. Ricci, S. Snyder, B. E. Paden, J. R. Boston, M. A. Simaan, and J. F. Antaki, "In vitro evaluation of multiobjective hemodynamic control of a heart-assist pump," *Amer. Soc. Artif. Internal Organs (ASAIO) J.*, vol. 51, pp. 329–335, 2005.

[11] K. Ohuchi, D. Kikugawa, K. Takahashi, M. Uemura, M. Nakamura, T. Murakami, T. Sakamoto, and S. Takatani, "Control strategy for rotary blood pumps," *Artif. Organs*, vol. 25, no. 5, pp. 366–370, 2001.

[12] M. Nakamura, T. Masuzawa, E. Tatsumi, Y. Taenaka, T. Nakamura, B. Zhang, T. Nakatani, H. Takano, and T. Ohno, "The development of a control method for a total artificial heart using mixed venous oxygen saturation," *Artificial Organs*, vol. 23, no. 3, pp. 235–241, 1999.

[13] G. A. Giridharan, M. Skliar, D. B. Olsen, and G. M. Pantalos, "Modeling and control of a brushless DC axial flow ventricular assist device," *Amer. Soc. Artif. Internal Organs (ASAIO) J.*, vol. 48, pp. 272–289, 2002.

[14] A. Ferreira, S. Chen, D. G. Galati, M. A. Simaan, and J. F. Antaki, "A dynamical state space representation of a feedback controlled rotary left ventricular assist device," in *Proc. 2005 ASME Int. Mech. Eng. Congr.*, Orlando, FL, Nov. 5–11, 2005, Paper IMECE2005-80973.

[15] A. Ferreira, M. A. Simaan, J. R. Boston, and J. F. Antaki, "A nonlinear state space model of a combined cardiovascular system and a rotary pump," in *Proc. 44th IEEE Conf. Decision Contr. Eur. Contr. Conf.*, Seville, Spain, Dec. 12–15, 2005, pp. 897–902.

[16] D. S. Breitenstein, "Cardiovascular modeling: The mathematical expression of blood circulation," M.S. thesis, Univ. Pittsburgh, PA, 1993.

[17] Y.-C. Yu, "Minimally invasive estimation of cardiovascular parameters," Ph.D. thesis, Univ. Pittsburgh, PA, 1998.

[18] Y.-C. Yu, J. R. Boston, M. A. Simaan, and J. F. Antaki, "Estimation of systemic vascular bed parameters for artificial heart control," *IEEE Trans. Autom. Contr.*, vol. 43, no. 6, pp. 765–778, Jun., 1998.

[19] H. Suga and K. Sagawa, "Instantaneous pressure-volume relationships and their ratio in the excised, supported canine left ventricle," *Circulatory Res.*, vol. 35, no. 1, pp. 117–126, 1974.

[20] N. Stergiopulos, J. Meister, and N. Westerhof, "Determinants of stroke volume and systolic and diastolic aortic pressure," *Amer. J. Physiol.*, vol. 270, no. 6, pp. H2050–H2059, 1996.

[21] A. C. Gyton and J. E. Hall, *Textbook of Medical Physiology*, 9th ed. Philadelphia, PA: W.B. Saunders, 1996.

[22] S. Choi, J. R. Boston, D. Thomas, and J. F. Antaki, "Modeling and identification of an axial flow pump," in *Proc. 1997 Amer. Contr. Conf.*, Albuquerque, NM, Jun. 4–6, 1997, pp. 3714–3715.

[23] H. Shima, J. Honigschnable, W. Trubel, and H. Thoma, "Computer simulation of the circulatory system during support with a rotary blood pump," *Trans. Amer. Soc. Artif. Organs*, vol. 36, no. 3, pp. M252–M254, 1990.

[24] A. Ferreira, M. A. Simaan, J. R. Boston, and J. F. Antaki, "Frequency and time-frequency based indexes for suction detection in rotary blood pumps," in *Proc. 2006 IEEE Int. Conf. Acoustics Speech Signal Process.*, Toulouse, France, May 14–19, 2006, vol. II, pp. 1064–1067.

[25] A. Ferreira, S. Chen, M. A. Simaan, J. R. Boston, and J. F. Antaki, "A discriminant-analysis-based suction detection system for rotary blood pumps," in *Proc. 28th IEEE Annu. Int. Conf. Eng. Med. Biol.*, New York, NY, 2006, pp. 5382–5385.

[26] G. Giridharan and M. Skliar, "Control strategy for maintaining physiological perfusion with implantable rotary blood pumps," *Artif. Organs*, vol. 27, pp. 639–648, 2003.

[27] G. Giridharan, G. Pantalos, S. Koenig, K. Gillars, and M. Skliar, "Physiological Control of Rotary Blood Pumps: An *in vitro* Study," *Amer. Soc. Artif. Internal Organs (ASAIO) J.*, vol. 50, pp. 403–409, 2004.

Marwan A. Simaan (S'69–M'72–SM'79–F'88) received the Ph.D. degree in electrical engineering from the University of Illinois at Urbana-Champaign in 1972.

He did postdoctoral work at the Coordinated Science Laboratory at the University of Illinois until 1974. He was a Research Engineer with Shell Development Company, Houston, TX, from 1974 to 1976. In 1976, he joined the Electrical Engineering Department at the University of Pittsburgh, Pittsburgh, PA, where he held the title of the Bell of PA/Bell Atlantic Professor. He served as chair of the department from 1991 to 1998. In 2008, he joined the University of Central Florida, Orlando, as the Florida 21st Century Chair and Distinguished Professor of Electrical Engineering and Computer Science. He has held research and consulting positions in industry including the English Electric Leo-Marconi Computers Ltd.; Bell Telephone Laboratories; Shell Development Company; Gulf R&D

Company; and ALCOA Laboratories. He has edited four books, written more than 300 articles in journals, books, conference proceedings and technical reports, and lectured extensively at national and international meetings. His research interests are mainly in the areas of control, optimization, and signal processing. For the past ten years, his research has focused on the control and performance optimization of biomedical devices and in particular the left ventricular assist device commonly known as LVAD.

Dr. Simaan is a Fellow of ASEE and AAAS and is member of the U.S. National Academy of Engineering (NAE). He received three IEEE Best Paper Awards (1985, 1988, and 1999) and the Distinguished Alumnus Award (1995) from the Department of Electrical and Computer Engineering at the University of Illinois at Urbana-Champaign. In 2007, he received the IEEE Education Society Achievement Award, and in 2008, he received the University of Illinois in Champaign-Urbana Award for Distinguished Service in Engineering. He currently serves and has served on the editorial or advisory boards of a number of journals including the *Proceedings of the IEEE*, the IEEE TRANSACTIONS ON CIRCUITS AND SYSTEMS II: EXPRESS BRIEFS, the IEEE TRANSACTIONS ON GEOSCIENCE AND REMOTE SENSING, the IEEE SYSTEMS JOURNAL, and the *Journal of Optimization Theory and Applications*. He is a Registered Professional Engineer in the Commonwealth of Pennsylvania.

James F. Antaki received the B.S. degree in mechanical and electrical engineering from Rensselaer Polytechnic Institute, Troy, NY, in 1985 and a the Ph.D. degree in mechanical engineering from the University of Pittsburgh, Pittsburgh, PA, in 1991.

He is a Professor of Biomedical Engineering with a courtesy appointment in Computer Science at Carnegie Mellon University, Pittsburgh, PA. He also holds academic positions in the departments of Surgery and Bioengineering, University of Pittsburgh. Over the past 20 years, he has conducted research in the field of prosthetic cardiovascular organs. He holds twelve patents related to artificial organs and four in other fields. His current research involves the development of circulatory support systems for children. He is also interested in studying methods of innovation and optimization of cardiovascular technologies.

In 1997, his team completed the development of a novel magnetically levitated turbodynamic blood pump, the *Streamliner*, which recorded the world's first in-vivo implant of such a device, and was granted an IEEE Controls Systems Technology Award in 2001.

Antonio Ferreira (S'05) received the B.S. and M.S. degrees in electrical engineering from Universidade Federal do Maranhao, Brazil, in 1994 and 1998, respectively, and the Ph.D. degree from University of Pittsburgh, Pittsburgh, PA, in 2007.

He was a Lecturer at the Department of Mathematics, Universidade Federal do Maranhao, Brazil, and served as a teaching assistant at the Department of Electrical and Computer Engineering at the University of Pittsburgh. His research interests include the areas of signal processing, pattern recognition, and the control of ventricular assist devices.

David G. Galati was born in 1978. He received the B.S., M.S., and Ph.D. degrees in electrical engineering from the University of Pittsburgh, Pittsburgh, PA, in 2000, 2002, and 2004, respectively.

Currently, he is working for the National Robotics Engineering Center at the Carnegie Mellon University Robotics Institute., Pittsburgh, PA. His primary focus is to apply innovative control techniques to achieve autonomous multi-agent collaboration and tightly coupled tactical behaviors. His interests also include classical control, optimization, game theory, multisignal decomposition, and the modeling and simulation of biological systems.

Shaohui Chen received the B.S. degree from Harbin Institute of Techonology, Harbin, China, in 1994, the M.S. degree from the China Academy of Launch Vehicle Technology, Nanyuan, China, in 2002, and the Ph.D. degree from University of Pittsburgh, Pittsburgh, PA, in 2006, all in electrical engineering.

From 1994 to 2002, he worked in the China Academy of Launch Vehicle Technology. He now works as a consultant with Mantaro Networks, Inc., Germantown, MD, on development of electrical systems. His research interest emphasizes signal processing in environment, bioengineering and digital communication areas.